Atmospheric
Chemistry
and Physics

Pyruvic acid in the boreal forest: gas-phase mixing ratios and impact on radical chemistry

Philipp G. Eger[1], Jan Schuladen[1], Nicolas Sobanski[1], Horst Fischer[1], Einar Karu[1], Jonathan Williams[1], Matthieu Riva[2,3], Qiaozhi Zha[2], Mikael Ehn[2], Lauriane L. J. Quéléver[2], Simon Schallhart[2], Jos Lelieveld[1], and John N. Crowley[1]

[1]Atmospheric Chemistry Department, Max Planck Institute for Chemistry, 55128 Mainz, Germany
[2]Institute for Atmospheric and Earth System Research/Physics, Faculty of Science, University of Helsinki,
Helsinki, 00014, Finland
[3]University of Lyon, Université Claude Bernard Lyon 1, CNRS, IRCELYON, 69626, Villeurbanne, France

Correspondence: John N. Crowley (john.crowley@mpic.de)

Abstract. Pyruvic acid ($CH_3C(O)C(O)OH$, 2-oxopropanoic acid) is an organic acid of biogenic origin that plays a crucial role in plant metabolism, is present in tropospheric air in both gas-phase and aerosol-phase, and is implicated in the formation of secondary organic aerosols (SOAs). Up to now, only a few field studies have reported mixing ratios of gas-phase pyruvic acid, and its tropospheric sources and sinks are poorly constrained. We present the first measurements of gas-phase pyruvic acid in the boreal forest as part of the IBAIRN (Influence of Biosphere–Atmosphere Interactions on the Reactive Nitrogen budget) field campaign in Hyytiälä, Finland, in September 2016. The mean pyruvic acid mixing ratio during IBAIRN was 96 pptv, with a maximum value of 327 pptv. From our measurements we estimated the overall pyruvic acid source strength and quantified the contributions of isoprene oxidation and direct emissions from vegetation in this monoterpene-dominated forested environment. Further, we discuss the relevance of gas-phase pyruvic acid for atmospheric chemistry by investigating the impact of its photolysis on acetaldehyde and peroxy radical production rates. Our results show that, based on our present understanding of its photochemistry, pyruvic acid is an important source of acetaldehyde in the boreal environment, exceeding ethane and propane oxidation by factors of ~ 10 and ~ 20.

1 Introduction

Organic acids play a crucial role in tropospheric chemistry. They influence the acidity of aerosols and cloud droplets and are involved in the formation of secondary organic aerosols (SOAs), thereby impacting air quality and climate (Kanakidou et al., 2005; Hallquist et al., 2009). Pyruvic acid, $CH_3C(O)C(O)OH$, the simplest α-keto acid, is omnipresent in plants, where it is central to the metabolism of isoprene, monoterpenes and sesquiterpenes (Eisenreich et al., 2001; Magel et al., 2006; Jardine et al., 2010), and is also found in tropospheric air, especially in the boundary layer of vegetated regions (see Sect. 1.3).

The boreal forest is one of the largest terrestrial biomes on Earth, covering about 10 % of its land surface and emitting large amounts of biogenic volatile organic compounds (VOCs) into the atmosphere (Kesselmeier and Staudt, 1999; Rinne et al., 2005; Hakola et al., 2012). It serves as an important global carbon reservoir (Bradshaw and Warkentin, 2015) and impacts the Earth's climate not only through forest–atmosphere carbon exchange but also via surface albedo, evapotranspiration, and formation of cloud condensation nuclei and SOA from gaseous biogenic precursors (Kulmala et al., 2004; Bonan, 2008; Sihto et al., 2011). Our work focuses on the first measurement and chemical impact of gas-phase pyruvic acid in a boreal forest environment.

1.1 Atmospheric sources of pyruvic acid

There are several known routes to the photochemical formation of gas-phase pyruvic acid in the troposphere. In clean air, pyruvic acid is generated during the photo-oxidation of isoprene via the ozonolysis of methyl vinyl ketone (MVK) and subsequent hydrolysis of the Criegee intermediates formed (Jacob and Wofsy, 1988; Grosjean et al., 1993; Paulot et al., 2009). Pyruvic acid is found in the photolysis (in air) of methylglyoxal (Raber and Moortgat, 1995), itself formed from the OH-initiated oxidation of several biogenic VOCs (Arey et al., 2009; Obermeyer et al., 2009) including monoterpenes (Yu et al., 1998; Fick et al., 2003). Pyruvic acid is also formed in the reactions of peroxy radicals generated in the oxidation of propane, acetone and hydroxyacetone (Jenkin et al., 1993; Warneck, 2005) and in the gas-phase photo-oxidation of aromatics in the presence of NO_x (Grosjean, 1984; Praplan et al., 2014).

In the condensed phase, the aqueous-phase oxidation of methylglyoxal leads to the formation of pyruvic acid (Stefan and Bolton, 1999). Biomass burning also results in the formation of pyruvic acid (Andreae et al., 1987; Helas et al., 1992), in which the heterogeneous photo-oxidation of particle-phase aromatics plays a role (Pillar et al., 2014, 2015; Pillar and Guzman, 2017; Pillar-Little and Guzman, 2018). The latter also results in the formation of a further oxo-carboxylic acid with the same molecular mass (3-oxopropanoic acid). Finally, pyruvic acid is believed to be directly emitted by vegetation as indicated by measurements of very high mixing ratios under oxidation-free conditions in a tropical rainforest biome (Jardine et al., 2010).

1.2 Atmospheric sinks of gas-phase pyruvic acid

Like other dicarbonyls, pyruvic acid has a UV-absorption spectrum that extends into the visible part of the electromagnetic spectrum (Horowitz et al., 2001) and is thus photolysed rapidly by actinic radiation. Experimental studies indicate that, in the gas-phase, pyruvic acid has a lifetime with respect to photolysis of a few hours (Grosjean, 1983; Winterhalter et al., 2001). In contrast, the rate constant for reaction of pyruvic acid with OH is slow (1.2×10^{-13} cm^3 molec.$^{-1}$ s^{-1}; IUPAC, 2019), and this may be considered a negligible sink with a lifetime of ~ 3 months (Mellouki and Mu, 2003). The photolysis of pyruvic acid proceeds mainly ($\sim 60\%$) via exothermic decarboxylation involving a five-membered transition state that decomposes into CO_2 and methylhydroxycarbene (CH_3COH), the latter rearranging to acetaldehyde (IUPAC, 2019). Other product channels observed are $CH_3CO + HOCO$ ($\sim 35\%$) and $CO + CH_3C(O)OH$ ($\sim 5\%$) (see Sect. 3.2 for more details). With a Henry's law constant of $\sim 3 \times 10^5$ M atm^{-1} (Staudinger and Roberts, 1996), pyruvic acid is highly soluble (due to formation of a germinal diol; Guzman et al., 2006) and wet and dry deposition and partitioning into the aerosol-phase are expected to be impor-

tant sinks, especially at high relative humidity, thus contributing to SOA formation (Carlton et al., 2006; Tan et al., 2012; Griffith et al., 2013; Reed Harris et al., 2014; Eugene and Guzman, 2017, 2019; Mekic et al., 2019).

1.3 Observations of ambient gas-phase pyruvic acid

Pyruvic acid was first observed by Andreae et al. (1987) in the Amazonas region (Brazil) as well as in the southern US, with most (85 %–93 %) found in the gas-phase, where mixing ratios ranged from 10 to 400 pptv. Andreae et al. (1987) reported the highest mixing ratios for the Amazon forest near the top of the forest canopy, which was considered consistent with formation from the oxidation of isoprene in the boundary layer and removal by dry deposition. Similarly, average daytime mixing ratios of pyruvic acid over central Amazonia of (25 ± 15) pptv (forest canopy) and (15 ± 15) pptv (free troposphere) (Talbot et al., 1990) were consistent with model predictions (Jacob and Wofsy, 1988) of pyruvic acid formation from isoprene degradation. Helas et al. (1992) found pyruvic acid mixing ratios up to 800 pptv in and above the equatorial African rainforest, which could not be attributed to isoprene oxidation, indicating additional sources. Pyruvic acid levels of up to 200 pptv in the rural continental atmosphere at a mountain top site over the eastern US were thought to originate from biogenic emissions and possibly photochemical production (Talbot et al., 1995). In regions influenced by anthropogenic emissions, pyruvic acid has been measured at mixing ratios of up to 500 pptv, whereby the diurnal profiles indicated a dominant photochemical source (Mattila et al., 2018), and it was present in an urban air mass in the Los Angeles Basin and New York (Khwaja, 1995; Veres et al., 2008). Very low mixing ratios (~ 1 pptv) of pyruvic acid were found in the marine boundary layer over the Atlantic Ocean (63° N to 39° S), confirming the importance of continental sources (Baboukas et al., 2000). Mixing ratios of pyruvic acid (up to 15 ppbv) were reported in an experimental tropical rainforest enclosure (Jardine et al., 2010) and were accompanied by isoprene levels exceeding 100 ppbv with other terpenoids up to ~ 10 ppbv. In the enclosure, photochemical production and loss of pyruvic acid are not important, and the high pyruvic acid mixing ratios were attributed to direct emissions.

Pyruvic acid is a potentially important but unexplored atmospheric component which is present in the gas-phase as well as in the aerosol phase (Andreae et al., 1987) and, along with other dicarbonyls, has been proposed to be a potentially important source of $CH_3C(O)O_2$ and HO_2 radicals in areas dominated by biogenic emissions (Crowley et al., 2018). So far, elevated pyruvic acid mixing ratios have only been observed in temperate or equatorial forests where isoprene emissions were large. In the following, we present the first gas-phase measurements of pyruvic acid in the boreal forest where isoprene levels (in September) were generally low and

investigate its impact on photochemical radical production in this environment.

2 Methods

The IBAIRN campaign (Influence of Biosphere–Atmosphere Interactions on the Reactive Nitrogen budget) took place in the boreal forest in Hyytiälä, Finland, in September 2016, during the summer–autumn transition. Measurements were performed at the "Station for Measuring Forest Ecosystem-Atmosphere Relations II" (SMEAR II) in Hyytiälä (61.846° N, 24.295° E, 180 m above sea level) in southern Finland (Hari and Kulmala, 2005), in a forested area that is characterised by large biogenic emissions and low NO_x concentrations (Williams et al., 2011; Crowley et al., 2018; Liebmann et al., 2018). The vegetation in the surrounding 50 km is dominated by Scots pine and Norway spruce and the site is only occasionally influenced by anthropogenic emissions, with the nearest city (Tampere) located ≈ 50 km to the south-west. A detailed description of the measurement site can be found elsewhere (Hari and Kulmala, 2005; Hari et al., 2013). Meteorological parameters including wind direction, wind speed, temperature, relative humidity and precipitation are continuously monitored at various heights on the 128 m SMEAR II tower and distributed via an online data exploration and visualisation tool for SMEAR stations (Junninen et al., 2009). Measurements of NO_3 radical reactivity, alkyl nitrates, highly oxygenated molecules (HOMs) and meteorological parameters during the IBAIRN campaign have recently been reported (Liebmann et al., 2018, 2019; Zha et al., 2018). Unless stated otherwise, the trace gases discussed in this paper were sampled from the centre of a high-volume-flow inlet ($10 \, m^3 \, min^{-1}$; 0.15 m diameter; 0.2 s residence time) made of stainless steel, the top of which was located at a height of 8 m above the ground (m a.g.). The top of the canopy around the clearing was at ~ 20 m.

2.1 CI-QMS measurement of pyruvic acid

Pyruvic acid was detected with a chemical ionisation quadrupole mass spectrometer (CI-QMS) equipped with an electrical radiofrequency (RF) discharge ion source, described in detail by Eger et al. (2019). The CI-QMS detected pyruvic acid as $CH_3C(O)C(O)O^-$ at a mass-to-charge ratio (m/z) of 87. The sensitivity was 4.8 Hz pptv^{-1} of pyruvic acid for a (typical) primary-ion count rate (at m/z 127) of $\sim 10^6$ Hz, which resulted in a detection limit (LOD) of 15 pptv (10 s; 2σ) or 4 pptv (10 min). The detection scheme is believed to be similar to the one reported for acetic acid (Eger et al., 2019) and involves the reaction of pyruvic acid with $I(CN)_2^-$ primary ions to initially form HCN + $I(CN)CH_3C(O)C(O)O^-$ (m/z 240), which then dissociates to $CH_3C(O)C(O)O^-$ (m/z 87) when a 20 V declustering voltage is applied in the collisional dissociation chamber.

The $I(CN)_2^-$ ion was not monitored continuously during the IBAIRN campaign, and the signal at m/z 87 was converted to a mixing ratio after normalisation to the ion count of the major primary ion, I^-. As the I and C atoms in $I(CN)_2^-$ stem from CH_3I, we expect the concentration of $I(CN)_2^-$ to be proportional to that of I^- (which was monitored continuously).

As detection of pyruvic acid during IBAIRN was not expected, the instrument was calibrated post-campaign by simultaneously monitoring the output of a diffusion source (98 % pyruvic acid, Sigma-Aldrich) with the CI-QMS and an infrared absorption spectrometer measuring CO_2 (LI-COR®) following the complete oxidation of pyruvic acid to three CO_2 molecules in air, using a palladium catalyst at 350 °C (Veres et al., 2010). A calibration curve is given in Fig. S1 of the Supplement. The CI-QMS sensitivity to pyruvic acid was found to be independent of relative humidity (RH) for RH > 20 %. In dry air the sensitivity drops to about 60 % of that observed with humidified air reflecting the importance of water clusters in the reaction with the primary ion.

A flow of 2.5 L min^{-1} (at standard temperature and pressure, STP) was drawn into the CI-QMS via a 3 m long 6.35 mm (outer diameter) PFA tubing and then into a 20 cm section of PFA that was heated to 200 °C, required for peroxyacetyl nitrate (PAN) detection (Eger et al., 2019). During calibration, we found no change in the pyruvic acid signal when the inlet was at either at room temperature or heated to 200 °C. We cannot completely rule out that some unknown secondary reactions at 200 °C may influence the pyruvic acid concentration during ambient measurements, though given the short inlet residence time (200 ms), we consider this to be unlikely.

A membrane filter (Pall Teflo, 2 µm pore) was placed between the high-volume inlet and CI-QMS sampling line to remove particles and was exchanged regularly to avoid accumulation of particulate matter. The ion molecule reactor was held at a pressure of 18.00 mbar (1 mbar = 100 Pa) and a declustering voltage of 20 V was applied in the collisional dissociation chamber.

The background signal at all masses monitored was determined by periodically passing ambient air (for 10 min) through a scrubber filled with steel wool where pyruvic acid was efficiently destroyed with the hot surfaces (120 °C). Owing to the high affinity of pyruvic acid for surfaces, even after 5–10 min of scrubbing, the signal did not go to zero (Fig. S2), which resulted in a background signal that covaried with the ambient signal at m/z 87. This is illustrated in Fig. S2 of the Supplement in which we show the raw signal at m/z 87 and the signal at the same mass when sampling via the scrubber. The background signal for m/z 87 (dashed red line in upper panel of Fig. S2) was therefore determined from measurements in which pyruvic acid mixing ratios were close to the detection limit during the early part of the campaign. This choice could be confirmed by examining the background signal when the inlet was overflowed with zero air. We have in-

creased the total uncertainty in the pyruvic acid mixing ratios to 30 % (of the mixing ratio) ± 20 pptv to take account of this.

The sensitivity of the CI-QMS to pyruvic acid can be accurately derived from laboratory-based calibrations. However, m/z 87 is subject to potential interferences owing to the limited mass resolution (~ 1 atomic mass unit, amu) of our quadrupole mass spectrometer. In the following, we discuss potential contributions of other trace gases to m/z 87 and examine the evidence that supports the assignment to (predominantly) pyruvic acid.

Analogous to the detection of PAN, $CH_3C(O)O_2NO_2$, as the acetate anion at m/z 59, we would expect the CI-QMS to detect C4 nitric anhydrides (peroxyisobutyric nitric anhydride, PiBN, and peroxy-n-butyric nitric anhydride, PnBN) at m/z 87 following thermal dissociation to a peroxy radical, which reacts with I^- to form $C_4H_7O_2^-$. As the CI-QMS detects the peroxy acids at the same m/z as the nitric anhydrides with the same carbon backbone, we would also expect to detect peroxyisobutyric acid and peroxy-n-butyric acid (Phillips et al., 2013). The CI-QMS was set up to measure PAN during IBAIRN and we therefore regularly added NO to our heated inlet to zero the signal from PAN and thus also PiBN and PnBN. The lack of signal modulation at m/z 87, while adding NO enables us to conclude that the contribution of PiBN and PnBN was insignificant, which is consistent with the low mixing ratios of PAN (the dominant nitric anhydride at this and most locations) observed during IBAIRN. Mixing ratios of PiBN and PnBN, generally associated with anthropogenically influenced air masses, are expected to be low at this site. Similarly, although differentiation between pyruvic acid and peroxyisobutyric/peroxy-n-butyric acid was not possible with our instrument, we expect the C4 peroxy acids to be present at very low concentrations in this pristine environment as their organic backbone is derived from organics of mainly anthropogenic origin (Gaffney et al., 1999; Roberts et al., 2002, 2003). Similar arguments help us to rule out a large contribution on m/z 87 from butanoic acid, which accompanies anthropogenic activity (e.g. traffic emissions; see Mattila et al., 2018) and would not acquire continuously high concentrations at this site. Assuming similar sensitivities for butanoic and acetic acid, i.e. 0.62 Hz pptv^{-1} (Eger et al., 2019), butanoic acid mixing ratios sometimes exceeding 2.5 ppbv would be required to account for the entire signal at m/z 87. In the absence of independent measurements of butanoic acid during IBAIRN, we can only conclude that it is unlikely to represent a significant fraction of the CI-QMS signal at m/z 87.

While the low resolution of the CI-QMS cannot differentiate between molecules of 87.008 amu with the formula $C_3H_3O_3^-$ (the anion from pyruvic acid) and molecules of 87.045 amu with the formula $C_4H_7O_2^-$ (the anion from PiBN, PnBN or butanoic acid) a second measurement of the exact mass of the anion detected at m/z 87 was provided by an Aerodyne high-resolution long time-of-flight chemical ionisation mass spectrometer (HR-L-ToF-CIMS), equipped with iodide (I^-) reagent ions (Lopez-Hilfiker et al., 2014; Riva et al., 2019). This instrument was located about 50 m away from the common inlet and sampled at a height of 1.5 m a.g. Although neither the instrument nor its inlet transmission was calibrated for pyruvic acid, the signals at m/z 214.921 ($C_3H_4O_3\cdot I^-$) and m/z 87.008 ($C_3H_3O_3^-$) confirmed the assignment of m/z 87 to a molecule with three C atoms and three O atoms and thus to pyruvic acid (2-oxopropanoic acid) or an isomer thereof such as 3-oxopropanoic acid, $HC(O)CH_2C(O)OH$ (also known as formyl acetic acid or malonaldehydic acid). Figure S3 shows that the dominant contribution to m/z 87 is an ion of formula $C_3H_3O_3^-$, which is a factor of ~ 10 larger than that assigned to $C_4H_7O_2^-$. The HR-L-ToF-CIMS, which was operated under conditions that minimised declustering, also identified a signal at m/z 214.921 that could be assigned to $C_3H_4O_3\cdot I^-$, which was about a factor of 10 higher than for the fragment at m/z 87.008. The correlation coefficient between both signals was 0.77, the deviation from unity likely being related to different responses to ambient relative humidity for formation and detection of the cluster and fragment. Pyruvic acid has been detected previously using a HR-L-ToF-CIMS (Lee et al., 2014), whereby a strong dependence of the sensitivity on the relative humidity was observed. If the same factors apply to the instrument used during IBAIRN, a significant change in sensitivity (up to a factor of 2) would have been observed over the course of the diel cycle when RH varied, for example, from 50 % at noon to 100 % at night. One might also expect a reduction in inlet transmission for this soluble, sticky trace gas at high relative humidity. As we have reported previously from the IBAIRN campaign (Liebmann et al., 2018) differences in mixing ratios of trace gases measured using the inlet at 8 m (e.g. CI-QMS) and that at 1.5 m (e.g. HR-L-ToF-CIMS) were large, especially for soluble trace gases, displayed different diel profiles due to the impact of ground-level fog in the evenings at the lower level. For these reasons, the uncalibrated HR-L-ToF-CIMS signal is used only to support the identification of pyruvic acid at m/z 87. We cannot rule out that 3-oxopropanoic acid contributed to our CI-QMS signal at m/z 87 (or the HR-L-ToF-CIMS signal at m/z 87.008). However, as 3-oxopropanoic acid has only been observed in the particle phase and is associated with air masses impacted by biomass burning (Pillar and Guzman, 2017) our assumption that pyruvic acid is the dominant contributor to the signal at m/z 87 during IBAIRN appears justified.

2.2 Other trace gases and meteorological parameters

In addition to pyruvic acid, the CI-QMS also measured mixing ratios of PAN, SO_2, HCl, and a combined signal due to acetic and peracetic acid. These measurements are described in Eger et al. (2019).

Measurements of O_3, NO, NO_2, VOCs and meteorological parameters (T, RH, wind speed and direction, photol-

ysis rate coefficients, and ultraviolet B – UVB – radiation) during IBAIRN have recently been described in detail (Liebmann et al., 2018, 2019). Briefly, O_3 was measured by a commercial ozone monitor (2B Technologies, Model 202) based on optical absorption spectroscopy with a LOD of 3 ppbv (10 s) and a total uncertainty of 2 % ±1 ppbv. NO was monitored using a chemiluminescence detector (CLD 790 SR, ECO Physics, Dürnten, Switzerland) with a LOD of 5 pptv (60 s) and a measurement uncertainty of 20 %. The NO_2 dataset was provided by a five-channel thermal dissociation cavity ring-down spectrometer (TD-CRDS) with a LOD of 60 pptv (60 s) and a total uncertainty of 6 % (Sobanski et al., 2016). CO was measured by a quantum cascade laser spectrometer with a total uncertainty of < 20 %. VOC measurements (isoprene and monoterpenes) were performed with a gas chromatograph (GC) (Agilent 7890B) coupled with an atomic emission detector (JAS AED III, Moers, Germany) with an accuracy of 5 % (see Supplement of Liebmann et al., 2018). The GC-AED provides useful information on the contribution of α-pinene, β-pinene, Δ-3-carene, camphene and d-limonene to the sum of monoterpenes. Isoprene and total monoterpenes were additionally measured with a proton transfer reaction time-of-flight mass spectrometer (PTR-TOF 8000, Ionicon Analytik GmbH) (Jordan et al., 2009; Graus et al., 2010), which was located about 170 m away in dense forest, sampling at a height of 2.5 m a.g. As the PTR-ToF-MS provides a higher temporal resolution than the GC-AED ($\sim$ 1 data point per hour), we used this dataset to investigate potential covariations of pyruvic acid with isoprene and total monoterpenes, bearing in mind that the mixing ratios of monoterpenes observed at the two locations sometimes differ owing to an inhomogeneous distribution of sources and poor mixing within the canopy (Liebmann et al., 2018).

Temperature and relative humidity were measured at the common inlet as well as on the nearby SMEAR II tower at a height of 8 m a.g. Wind direction and speed were measured on the SMEAR II tower (8 m) along with UVB radiation (280–320 nm; Solar Light SL501A radiometer, 18 m); the data were provided via SmartSMEAR (Junninen et al., 2009). Photolysis rate coefficients (J_{NO_2}, J_{NO_3} and J_{pyr}) were calculated from actinic flux measurements at 35 m height using a spectral radiometer (METCON GmbH) and from evaluated cross sections and quantum yields (Burkholder et al., 2015). OH radical concentrations were calculated from the correlation of ground-level OH measurements with UVB radiation intensity (in units of watts per square metre) at the Hyytiälä site (Rohrer and Berresheim, 2006; Petäjä et al., 2009; Hellén et al., 2018). To account for gradients in OH between ground level and canopy height (Hens et al., 2014), the calculated, ground level OH concentrations (50 % uncertainty) were multiplied by a factor of 2.

3 Results and discussion

The IBAIRN campaign was characterised by relatively high daytime temperatures for September and frequent nighttime temperature inversions, which were accompanied by drastic losses of ozone and an increase in monoterpenes in a very shallow nocturnal boundary layer of $\sim$ 35 m compared to $\sim$ 570 m during daytime (Hellén et al., 2018; Liebmann et al., 2018, 2019; Zha et al., 2018). The high variability in the boundary layer height over the course of the diel cycle dictated the diel pattern of many of the trace gases. A time series of pyruvic acid mixing ratios together with isoprene, monoterpenes, NO_x, O_3 and meteorological parameters is presented in Fig. 1. Pyruvic acid was present at mixing ratios of 17–327 pptv, with a mean value of 96 ± 45 pptv and a median of 97 pptv (based on 1740 data points at 10 min resolution). During two periods of a few hours duration (9–10 September), operations from a nearby sawmill were apparent as elevated monoterpene mixing ratios (Eerdekens et al., 2009; Williams et al., 2011; Hakola et al., 2012). The influence of the sawmill could be confirmed by examining 48 h back trajectories (HYSPLIT; Draxler and Rolph 2011). These periods are highlighted (grey shading) in Fig. 2, which focuses on a section of the campaign in which the pyruvic acid mixing ratios were rather variable, and we compare them with those of isoprene and monoterpenes. There is apparent covariation of pyruvic acid with isoprene and monoterpenes, the nighttime maxima resulting from emissions into the very shallow boundary layer. As we discuss later, the mixing ratios of highly soluble pyruvic acid will be more strongly influenced by deposition or scavenging by aqueous particles than isoprene or monoterpenes so that there is no reason to expect continuously high correlation between these trace gases as meteorological conditions change.

Owing to its large affinity for surfaces, sharp changes in pyruvic acid mixing ratios (timescales of minutes) will be smeared out over timescales of tens of minutes because of adsorption and desorption on the inlet line and the filter and filter holder. We do not expect that this will significantly impact the pyruvic acid time series over the course of the diel cycle.

No correlation ($R^2 < 0.1$) was found between pyruvic acid mixing ratios and actinic flux, temperature or relative humidity, and there was no indication of elevated pyruvic acid mixing ratios in anthropogenically influenced air masses, marked by high levels of NO_x. Below we show that known photochemical sources of pyruvic acid are insufficiently strong to account for the observed mixing ratios.

3.1 Sources and sinks of pyruvic acid

Figure 3 shows a diel profile of median pyruvic acid, isoprene and monoterpenes, for the whole IBAIRN campaign. Diel mixing ratios of OH, O_3 and the rate constant for photolysis of pyruvic acid (J_{pry}) are displayed in Fig. 4. The
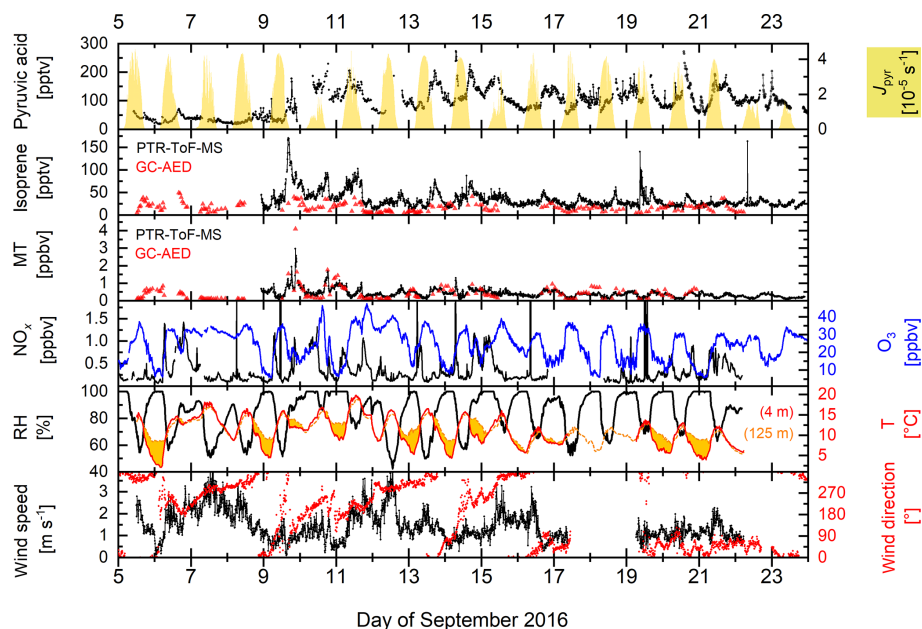
Figure 1. Time series of pyruvic acid mixing ratios, photolysis rate (J_{pyr}), isoprene and monoterpenes (PTR-ToF-MS, GC-AED), NO_x ($NO_2 + NO$), O_3, RH, temperature (at 4 and 125 m, with nighttime inversions indicated by the coloured area), and wind speed and direction during the IBAIRN campaign.
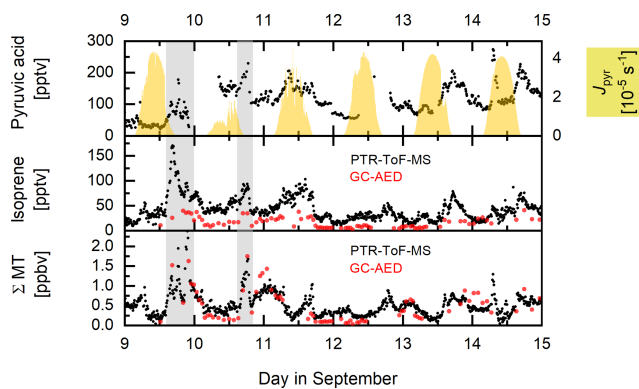
Figure 2. Times series of pyruvic acid, isoprene and total monoterpenes (ΣMT). The shaded areas represent periods where the site was impacted by sawmill activity.
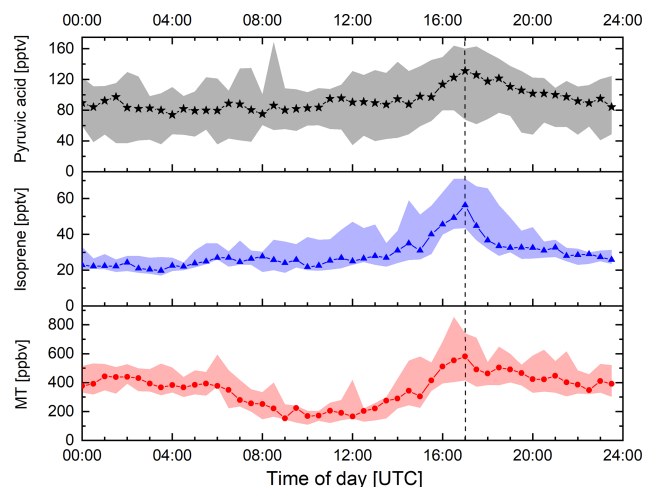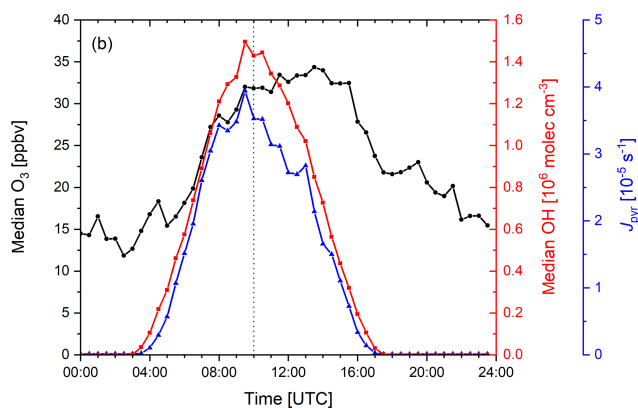

Figure 3. Diel profiles of median mixing ratios of pyruvic acid, isoprene and monoterpenes (MT) during the IBAIRN campaign. The shaded area represents the 25th and 75th percentiles.

diel profile of pyruvic acid follows neither the actinic flux (or OH) nor O_3 (markers of photochemical activity) but has features in common with isoprene and total monoterpenes including a rapid increase between 15:00 and 17:00 UTC prior to a decrease in mixing ratio towards midnight. The diel patterns observed are mainly determined by the interplay between production/emission rate (dependent on temperature and light), the boundary layer height, and chemical and physical loss processes, such as dry deposition. On nights impacted by strong temperature inversions, the 17:30 UTC maximum was more pronounced, indicating the important role of boundary layer dynamics. The diel profile of pyru-

vic acid bears more resemblance to that of isoprene than to that of monoterpenes, which may indicate that the emission rate is sensitive to both temperature and levels of photosynthetically active radiation.

It is also conceivable that pyruvic acid is emitted not only by the same vegetation as isoprene or monoterpenes but also that emissions from undergrowth and decaying vegetation may play a role during the autumn. Enclosure experiments would be useful to clarify this.

Figure 4. Diel profiles of median mixing ratios of O_3, OH and J_{pyr} (calculated with a quantum yield of 0.2) during the IBAIRN campaign.

Combining measurements of the mixing ratios of isoprene, monoterpenes and pyruvic acid with calculated loss rates of each enables rough estimation of the source strength of pyruvic acid relative to that of monoterpenes or isoprene. The rate constant for reaction with of OH with pyruvic acid is low (Mellouki and Mu, 2003) so that its main chemical sink during the day is photolysis, with a photolysis rate coefficient of $J_{pyr} \sim 4 \times 10^{-5}\,\mathrm{s}^{-1}$ at solar noon ($\sim 10{:}00$ UTC; see Fig. 4). The high solubility of pyruvic acid (see above) implies that dry deposition will be an important sink. To assess its impact on pyruvic acid lifetimes we use the daytime deposition velocity for H_2O_2, $V_{dep} = (8 \pm 4)\,\mathrm{cm\,s}^{-1}$, previously reported for this location (Crowley et al., 2018). The rationale for using the deposition velocity for H_2O_2 as surrogate for pyruvic acid is a similar solubility ($H_{H_2O_2} \sim 1 \times 10^5\,\mathrm{M\,atm}^{-1}$). Using $k_{dep} = V_d h^{-1}$ and a boundary layer height (h) of 570 m at solar noon (Hellén et al., 2018) results in a loss rate constant for deposition of $k_{dep} = 1.6 \times 10^{-4}\,\mathrm{s}^{-1}$. We also consider the loss of pyruvic acid via heterogeneous uptake to particles, which can be assessed via Eq. (1).

$$k_{het} = \frac{\gamma\,\overline{c}\,A}{4}, \tag{1}$$

where γ is the uptake coefficient, A the aerosol surface area density (in square centimetres per cubic centimetre), $\overline{c}$ the average thermal velocity (in centimetres per second). Using, the mean aerosol surface area observed during IBAIRN of $2 \times 10^{-7}\,\mathrm{cm^2\,cm^{-3}}$ (Liebmann et al., 2019), with $\overline{c} = 2.65 \times 10^4\,\mathrm{cm\,s}^{-1}$ at 290 K and an uptake coefficient of 0.06 reported for the uptake to aqueous surfaces (Eugene et al., 2018) we derive $k_{het} = 8 \times 10^{-5}\,\mathrm{s}^{-1}$.

The overall loss rate (photolysis + deposition heterogeneous loss) of pyruvic acid is then $L_{pyr} = 2.8 \times 10^{-4}\,\mathrm{s}^{-1}$, corresponding to a lifetime of ~ 1 h. We emphasise that the calculated lifetime (and thus the source strength we derive below) are very sensitive to the estimated deposition rate and are thus subject to major uncertainties. In addition, the ap-

propriate uptake coefficient may be less than its value on pure water if the aerosol contains a large mass fraction of organic material, which will reduce the rate of accommodation of pyruvic acid at the surface as has been seen for other trace gases e.g. N_2O_5 (Folkers et al., 2003; Abbatt et al., 2012).

To calculate the lifetime and the emission rates (at 10:00 UTC) of isoprene and monoterpenes, we assumed that reaction with OH (at $1.5 \times 10^6\,\mathrm{molec.\,cm}^{-3}$; see Fig. 4) and O_3 are the main loss processes and that dry deposition is insignificant. For isoprene, we used the rate coefficients evaluated by IUPAC (Atkinson et al., 2006; IUPAC, 2019); for the monoterpenes we used the rate coefficients (also from IUPAC) for α-pinene, which constituted, on average, more than 50 % of the overall monoterpene mixing ratio. This resulted in a loss rate constant for isoprene (L_{isop}) and monoterpenes (L_{MT}) of $1.4 \times 10^{-4}\,\mathrm{s}^{-1}$ for both trace gases, corresponding to a lifetime of ~ 2 h.

Assuming steady state (ss) for all three trace gases, the source strength for pyruvic acid (S_{pyr}) relative to the emissions rates of isoprene (E_{isop}) or monoterpenes (E_{MT}) is given by Eqs. (1) and (2), where [pyr], [isop] and [MT] are the measured mixing ratios of pyruvic acid, isoprene and monoterpenes.

$$\frac{S_{pyr}}{E_{isop}} = \frac{[pyr]_{ss}L_{pyr}}{[isop]_{ss}L_{isop}} \tag{2}$$

$$\frac{S_{pyr}}{E_{MT}} = \frac{[pyr]_{ss}L_{pyr}}{[MT]_{ss}L_{MT}} \tag{3}$$

Taking the diel-averaged mixing ratios of pyruvic acid, isoprene and monoterpenes at 10:00 UTC (83, 22 and 168 pptv) and the loss terms calculated above, results in a pyruvic acid source strength relative to isoprene and monoterpenes (based on the PTR-ToF-MS measurements) of 7 and 0.9, respectively (Table 1). When using the (low-time-resolution) GC-AED dataset for isoprene and monoterpenes, these values increase to 14 and 1.3, respectively.

In steady state, using $S_{pyr} = [pyr]_{ss}L_{pyr}$, the pyruvic acid source strength needed to account for the observed 10:00 UTC mixing ratios of ~ 80 pptv is $S_{pyr} = 84\,\mathrm{pptv\,h}^{-1}$ (or $12\,\mathrm{pptv\,h}^{-1}$ when neglecting dry deposition and heterogeneous uptake to particles; see Table 1). These values can be compared with the production rate of pyruvic acid from the photochemical oxidation of isoprene, which we calculate to be $0.02\,\mathrm{pptv\,h}^{-1}$, orders of magnitude too small to explain the pyruvic acid mixing ratios observed. The bases for this calculation were measured isoprene and O_3 mixing ratios and the results from chamber experiments (Grosjean et al., 1993; Paulot et al., 2009) that report a pyruvic acid yield from isoprene oxidation of ~ 2 %. Pyruvic acid is also a product of the ozonolysis of methyl vinyl ketone (MVK), with a yield of ~ 5 % (Grosjean et al., 1993). In order to explain the observed pyruvic acid mixing ratios by the production rate from MVK alone would require 16 ppbv of MVK, which is a fac-

Table 1. Calculated source strength of pyruvic acid (S_{pyr}), production rate from isoprene $+ O_3$ ($P_{pyr(isop+O_3)}$), and emission rates of isoprene (E_{isop}) and monoterpenes (E_{MT}) at solar noon.

Source strength (pptv h^{-1})	$J_{pyr} = 4 \times 10^{-5}\,s^{-1}$ $k_{dep} = 16 \times 10^{-5}\,s^{-1}$ $k_{het} = 8 \times 10^{-5}\,s^{-1}$	$J_{pyr} = 4 \times 10^{-5}\,s^{-1}$ $k_{dep} = 0$ $k_{het} = 0$
S_{pyr}	84	12
$P_{pyr(isop+O_3)}$	0.02	
	PTR-ToF-MS	GC-AED
E_{isop}	12	6
E_{MT}	94	65

Notes: S_{pyr} is the net source strength (emission rate + production rate) of pyruvic acid based on measured mixing ratios at solar noon, the assumption of steady state, and the fact that photolysis (J_{pyr}), deposition (k_{dep}) and heterogeneous uptake (k_{het}) are the only significant loss processes. The net source strength is derived for two different scenarios as discussed in the text. $P_{pyr(isop+O_3)}$ is the rate of photochemical production of pyruvic acid from isoprene oxidation. The net isoprene and net monoterpene emission rates (E_{isop} and E_{MT}) were calculated using their mixing ratios and considering the reactions with OH and O_3 as the only relevant loss terms. Emission rates are shown for both VOC datasets (PTR-ToF-MS and GC-AED).

tor ~ 60 more than observed at this site during September (Hakola et al., 2003) and clearly not feasible.

As the degradation of monoterpenes is not expected to generate pyruvic acid (Vereecken et al., 2007; IUPAC, 2019), we conclude that, in the boreal forest around Hyytiälä, the main source of pyruvic acid is direct emission from the biosphere and not photochemical production via reactions of OH or O_3. This is consistent with the measurements of Jardine et al. (2010) who reported high mixing ratios of pyruvic acid resulting from direct emission in an O_3 and OH-free environment. In contrast, Mattila et al. (2018) provided convincing evidence for photochemical production of pyruvic acid resulting in a mean mixing ratio of 180 pptv, maximising with photochemical activity. Mattila et al. (2018) also observed a strong reduction in the mixing ratio of pyruvic acid with height within the boundary layer due to dry deposition and found no evidence for strong surface emissions. As described above, dry deposition will also have impacted on the pyruvic acid mixing ratios observed at Hyytiälä, though in the absence of vertical profiles or flux measurements it is difficult to assess rigorously its impact during day or night. The differences between the summertime measurements of Mattila et al. (2018) and the present work are very likely related to the starkly contrasting environments. The IBAIRN campaign was conducted in the remote boreal forest in autumn, whereas Mattila et al. (2018) made their summertime measurements over an 8 d period in a region with sparse vegetation and with significant anthropogenic influence from traffic, oil and natural gas operations, and livestock, and NO_x levels of several parts per billion by volume and concluded that pyruvic acid was generated photochemically from aromatics emitted by automobiles.

3.2 Role of gas-phase pyruvic acid in the troposphere

In this section, we assess the potential role of pyruvic acid as source of radicals and other reactive trace gases in the boreal forest. Figure 5 provides an overview of the sources and sinks of pyruvic acid. The dominant photochemical loss process of pyruvic acid is its photolysis. Experimental data on its UV cross sections and photodissociation quantum yields have recently been evaluated by the IUPAC panel (IUPAC, 2019). The thermodynamically accessible dissociation pathways are listed below (Reactions R1–R3).

$$CH_3C(O)C(O)OH + h\nu \rightarrow CH_3CHO + CO_2 \quad (R1)$$
$$\rightarrow CH_3CO + HOCO \quad (R2)$$
$$\rightarrow CH_3C(O)OH + CO \quad (R3)$$
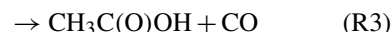
Photolysis of gas-phase pyruvic acid in the actinic region ($\lambda > 310$ nm) results mainly in the formation of acetaldehyde $CH_3CHO + CO_2$ (Reaction R1) with a yield of 60 %. The second most important channel (Reaction R2, with a yield of 35 %) leads to formation of organic radical fragments which react with O_2 to form the peroxy radicals $CH_3C(O)O_2$ and HO_2 (Reactions R4 and R5).

$$CH_3CO + O_2 + M \rightarrow CH_3C(O)O_2 + M \quad (R4)$$
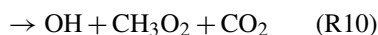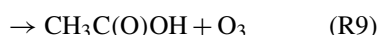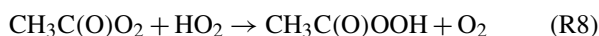$$HOCO + O_2 \rightarrow HO_2 + CO_2 \quad (R5)$$
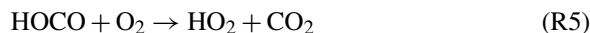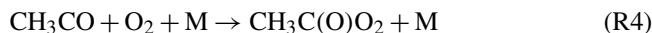
Acetaldehyde (formed in Reaction R1) is an air pollutant which plays an important role in tropospheric chemistry as a source of PAN (Roberts, 1990), peracetic acid (PAA) (Phillips et al., 2013; Crowley et al., 2018), HO_x radicals (Singh et al., 1995) and ultimately, via methyl peroxy radical oxidation, HCHO (Lightfoot et al., 1992). Based on campaign-median pyruvic acid mixing ratios and photolysis rates measured during IBAIRN (see Figs. 3 and 4), we calcu-

late an acetaldehyde production rate of $P_{CH_3CHO} = 0.6 J_{pyr} \times$ [pyr] $= 6.3$ pptv h^{-1} at local noon (Table 2; Fig. S4).

On a global scale the main source of acetaldehyde is OH-initiated photochemical production from alkanes, alkenes, ethanol and isoprene, with alkanes accounting for about one-half of the total production of 128 Tg a^{-1} (Millet et al., 2010). Minor sources are direct biogenic emissions (23 Tg a^{-1}), anthropogenic emissions (2 Tg a^{-1}) and biomass burning (3 Tg a^{-1}). As alkanes were not measured during IBAIRN we estimate the mixing ratios of the three most abundant alkanes (ethane, propane and n-butane) from monthly averages measured at Pallas and Utö (both Finland) for the years 1994–2003 (Hakola et al., 2006), which are consistent with measurements at Pallas in 2012 reported by Hellén et al. (2015). Combining mean (September) mixing ratios of 1000 pptv of ethane, 250 pptv of propane and 150 pptv of n-butane with OH rate coefficients of $k_{OH+ethane} = 2.4 \times 10^{-13}$ cm^3 molec.$^{-1}$ s^{-1}, $k_{OH+propane} = 1.1 \times 10^{-12}$ cm^3 molec.$^{-1}$ s^{-1} and $k_{OH+n-butane} = 2.35 \times 10^{-12}$ cm^3 molec.$^{-1}$ s^{-1} at 298 K (IUPAC, 2019) and acetaldehyde yields (at 0.1 ppbv of NO$_x$) of 0.50, 0.24 and 0.69 (Millet et al., 2010), results in a total CH$_3$CHO production rate from OH + alkanes of 2.2 pptv h^{-1} at local noon (Table 2). Figure S4 indicates how these production rates vary over the diel cycle. From these calculations we conclude that emission and subsequent photolysis of pyruvic acid is likely an important source of CH$_3$CHO in this environment and may impact our current understanding of the acetaldehyde budget (Millet et al., 2010) in forested regions in general.

The dominant sink of CH$_3$CHO is the reaction with OH (Reaction R6) with a rate constant of 1.5×10^{-11} cm^3 molec.$^{-1}$ s^{-1} (IUPAC, 2019) to form the CH$_3$CO radical. This then reacts in air (Reaction R4) to form CH$_3$C(O)O$_2$, which is the precursor of PAN (CH$_3$C(O)O$_2$NO$_2$, Reaction R7), peracetic acid (CH$_3$C(O)OOH, Reaction R8), acetic acid (CH$_3$C(O)OH, Reaction R9) and CH$_3$O$_2$ (Reactions R10 and R11), and which can recycle OH (Reaction R10).

$$OH + CH_3CHO(+O_2) \rightarrow CH_3C(O)O_2 + H_2O \quad (R6)$$

$$CH_3C(O)O_2 + NO_2 + M \rightarrow CH_3C(O)O_2NO_2 + M \quad (R7)$$

$$CH_3C(O)O_2 + HO_2 \rightarrow CH_3C(O)OOH + O_2 \quad (R8)$$

$$\rightarrow CH_3C(O)OH + O_3 \quad (R9)$$

$$\rightarrow OH + CH_3O_2 + CO_2 \quad (R10)$$

$$CH_3C(O)O_2 + NO(O_2) \rightarrow CH_3O_2 + CO_2 + NO_2 \quad (R11)$$

The second most important photolysis channel for pyruvic acid is Reaction (R2), which leads to formation of HO$_2$ and CH$_3$C(O)O$_2$. These radicals play a crucial role in photochemical ozone production (Fishman and Crutzen, 1978), in the recycling of OH (in the presence and absence of NO$_x$) and, as described above, in PAN formation.

The production rate (10:00 UTC) of HO$_2$ and CH$_3$C(O)O$_2$ from pyruvic acid photolysis is given by $P_{HO_2} = P_{CH_3CO_3} = 0.35 J_{pyr} \times$ [pyr] and is equal to 4 pptv h^{-1}. This value is roughly equivalent to the production rate of CH$_3$C(O)O$_2$ from the OH-initiated acetaldehyde oxidation (the major source of this radical) assuming typical values of 100 pptv CH$_3$CHO and 1.5×10^6 OH molec. cm^{-3} and using $k_{OH+CH_3CHO} = 1.5 \times 10^{-11}$ cm^3 molec.$^{-1}$ s^{-1} (IUPAC, 2019). We therefore conclude that pyruvic acid photolysis in this environment is an important source of the CH$_3$C(O)O$_2$ radical both directly (Reactions R2 and R4) and via acetaldehyde formation (Reactions R1 and R6).

Taking median O$_3$ and CO mixing ratios (at 10:00 UTC) found in IBAIRN, we can easily show that the rate of HO$_2$ formation (4 pptv h^{-1}) from pyruvic acid photolysis (Reactions R2 and R5) is minor compared to that from OH + O$_3$ of 12 pptv h^{-1} (with $k_{OH+O_3} = 7.3 \times 10^{-14}$ cm^3 molec.$^{-1}$ s^{-1}) and OH+CO of 100 pptv h^{-1} (with $k_{OH+CO} = 2.1 \times 10^{-13}$ cm^3 molec.$^{-1}$ s^{-1}) (IUPAC, 2019). It is also negligible compared to the total HO$_2$ production rate of 100–600 pptv h^{-1} previously derived in this environment (albeit in summer) via measurement of HO$_x$ (Hens et al., 2014).

So far, to calculate the photo-dissociation rate constant for pyruvic acid (J_{pyr}) we have used the IUPAC recommendation of an overall quantum yield of 0.2 at atmospheric pressure. There are however several inconsistencies in the experimental datasets on pyruvic acid photolysis, with two groups reporting quantum yields that are a factor of ~ 4 larger at this pressure (Berges and Warneck, 1992; Reed Harris et al., 2017). If these large quantum yields were to be correct, the calculated production rates of CH$_3$CHO and CH$_3$C(O)O$_2$ would increase by a factor of 4 (see Table 2) so that $P_{CH_3CHO} \sim 25$ pptv h^{-1} (Table 2). Moreover, Reed Harris et al. (2017) report much lower yields of CH$_3$CHO, and suggest that other processes may compete with rearrangement of the methylhydroxycarbene (CH$_3$COH) necessary to form acetaldehyde. They propose that in air, initially formed methylhydroxycarbene may react with O$_2$ to form CH$_3$CO and HO$_2$. If this is correct, the intermediate step (Reaction R6) in which OH reacts with acetaldehyde to form CH$_3$C(O)O$_2$ in air is bypassed so that pyruvic acid photolysis would be an even more important source of PAN. This alternative fate of the methylhydroxycarbene radical is depicted with the dashed line in Fig. 5.

4 Conclusions

Mixing ratios of pyruvic acid of 17–327 pptv (mean of 96 ± 45 pptv) were measured in the boreal forest in Hyytiälä, southern Finland, during a field study in late summer (September 2016). Campaign-averaged diel profiles of pyruvic acid displayed similar features to those of monoterpenes and isoprene. Combining the mixing ratios of pyruvic acid

Table 2. Calculated production rates of acetaldehyde, HO_2 and $CH_3C(O)O_2$ from the photolysis of pyruvic acid at solar noon.

CH_3CHO production rate $(pptv\,h^{-1})$	$J_{pyr} = 4 \times 10^{-5}\,s^{-1}$	$J_{pyr} = 16 \times 10^{-5}\,s^{-1}$
Pyruvic acid $+ h\nu$	6.3	25.2
OH + ethane	0.6	0.6
OH + propane	0.3	0.3
OH + n-butane	1.3	1.3
HO_2 production rate $(pptv\,h^{-1})$		
Pyruvic acid $+ h\nu$	4	16
$OH + O_3$	12	12
OH + CO	100	100
$CH_3C(O)O_2$ production rate $(pptv\,h^{-1})$		
Pyruvic acid $+ h\nu$	4	16
$CH_3CHO + h\nu$	5	5

Notes: the production rates of CH_3CHO, HO_2 and $CH_3C(O)O_2$ from pyruvic acid photolysis are derived for two different values of J_{pyr}, using quantum yields of 0.2 and 0.8 (see text). The production rates of CH_3CHO formation from alkanes are based on estimated mixing ratios (see text). The production rate of HO_2 from the reaction of OH with O_3 and CO is based on calculated OH and measurements of O_3 and CO during IBAIRN. The production rate of $CH_3C(O)O_2$ from CH_3CHO was calculated using a mixing ratio of 100 pptv of acetaldehyde.
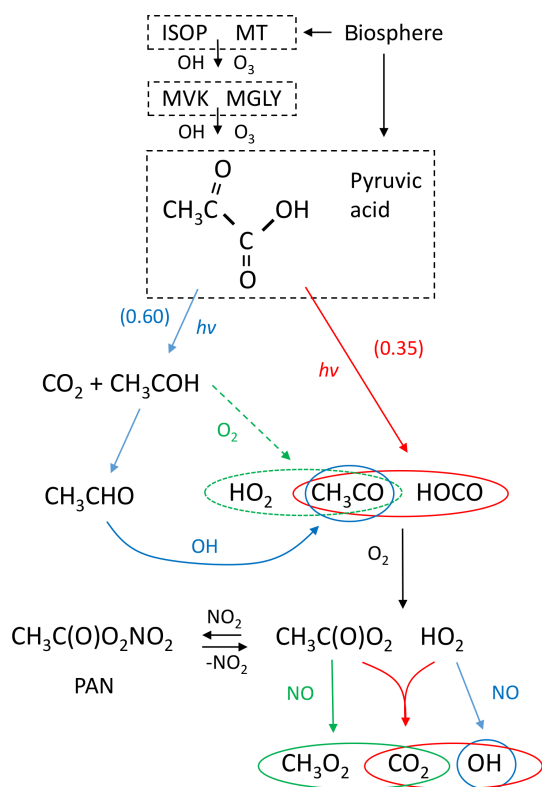
Figure 5. Sources of pyruvic acid and mechanism of formation of CH_3CHO, HO_2 and $CH_3C(O)O_2$ during its photolysis. ISOP: isoprene; MT: monoterpenes; MVK: methyl vinyl ketone; and MGLY: methylglyoxal. Numbers in parentheses indicate branching ratios. CH_3COH is the methylhydroxycarbene that is believed to mainly rearrange to form CH_3CHO.

with its loss terms enabled calculation of the source strength at solar noon of $\sim 80\,pptv\,h^{-1}$. There appears to be no known photochemical mechanism to generate pyruvic acid at this rate, and we suggest that pyruvic acid is, to a large extent, emitted directly from the biosphere. We show that pyruvic acid, at the mixing ratios observed in September, represents an important source of acetaldehyde and the acetyl peroxy radical, thus enhancing the formation of PAN, C_2 organic acids and CH_3O_2.

We conclude that, during late summer/autumn, pyruvic acid is an important biogenic VOC in the boreal forest which has previously received little attention. Further field and enclosure studies are necessary to quantify its emissions and role during other seasons and to better understand its sources and sinks (e.g. generation in $OH/O_3/NO_3$-initiated oxidation of terpenes and dry deposition rates) in the boreal forest as well as in other environments. To this end, co-located high-time-resolution measurements of mixing ratios and fluxes of terpenoids and pyruvic acid are necessary.

In addition, further laboratory studies are required to resolve discrepancies in the literature data on the pressure (and wavelength) dependence of both the overall photolysis quantum yield and the product distribution during pyruvic acid photolysis in the gas phase.

References

Abbatt, J. P. D., Lee, A. K. Y., and Thornton, J. A.: Quantifying trace gas uptake to tropospheric aerosol: recent advances and remaining challenges, Chem. Soc. Rev., 41, 6555–6581, https://doi.org/10.1039/c2cs35052a, 2012.

Andreae, M. O., Talbot, R. W., and Li, S. M.: Atmospheric measurements of pyruvic and formic acid, J. Geophys. Res.-Atmos., 92, 6635–6641, https://doi.org/10.1029/JD092iD06p06635, 1987.

Arey, J., Obermeyer, G., Aschmann, S. M., Chattopadhyay, S., Cusick, R. D., and Atkinson, R.: Dicarbonyl Products of the OH Radical-Initiated Reaction of a Series of Aromatic Hydrocarbons, Environ. Sci. Tech., 43, 683–689, https://doi.org/10.1021/es8019098, 2009.

Atkinson, R., Baulch, D. L., Cox, R. A., Crowley, J. N., Hampson, R. F., Hynes, R. G., Jenkin, M. E., Rossi, M. J., Troe, J., and IUPAC Subcommittee: Evaluated kinetic and photochemical data for atmospheric chemistry: Volume II – gas phase reactions of organic species, Atmos. Chem. Phys., 6, 3625–4055, https://doi.org/10.5194/acp-6-3625-2006, 2006.

Baboukas, E. D., Kanakidou, M., and Mihalopoulos, N.: Carboxylic acids in gas and particulate phase above the At-

lantic Ocean, J. Geophys. Res.-Atmos., 105, 14459–14471, https://doi.org/10.1029/1999jd900977, 2000.

Berges, M. G. M. and Warneck, P.: Product quantum yields for the 350 nm photodecomposition of pyruvic-acid in air, Ber. Bunsen Phys. Chem., 96, 413–416, https://doi.org/10.1002/bbpc.19920960334, 1992.

Bonan, G. B.: Forests and climate change: forcings, feedbacks, and the climate benefits of forests, Science, 320, 1444–1449, https://doi.org/10.1126/science.1155121 2008.

Bradshaw, C. J. and Warkentin, I. G.: Global estimates of boreal forest carbon stocks and flux, Global Planet. Change, 128, 24–30, https://doi.org/10.1016/j.gloplacha.2015.02.004, 2015.

Burkholder, J. B., Sander, S. P., Abbatt, J., Barker, J. R., Huie, R. E., Kolb, C. E., Kurylo, M. J., Orkin, V. L., Wilmouth, D. M., and Wine, P. H.: Chemical Kinetics and Photochemical Data for Use in Atmospheric Studies, Evaluation No. 18, JPL Publication 15-10, Jet Propulsion Laboratory, Pasadena, available at: http://jpldataeval.jpl.nasa.gov (last access: 23 March 2020), 2015.

Carlton, A. G., Turpin, B. J., Lim, H. J., Altieri, K. E., and Seitzinger, S.: Link between isoprene and secondary organic aerosol (SOA): Pyruvic acid oxidation yields low volatility organic acids in clouds, Geophys. Res. Lett., 33, L06822, https://doi.org/10.1029/2005GL025374, 2006.

Crowley, J. N. and Eger, P.: Pyruvic acid Dataset. IBAIRN campaign, Zenodo, https://doi.org/10.5281/zenodo.3600486, 2020.

Crowley, J. N., Pouvesle, N., Phillips, G. J., Axinte, R., Fischer, H., Petäjä, T., Nölscher, A., Williams, J., Hens, K., Harder, H., Martinez-Harder, M., Novelli, A., Kubistin, D., Bohn, B., and Lelieveld, J.: Insights into HO_x and RO_x chemistry in the boreal forest via measurement of peroxyacetic acid, peroxyacetic nitric anhydride (PAN) and hydrogen peroxide, Atmos. Chem. Phys., 18, 13457–13479, https://doi.org/10.5194/acp-18-13457-2018, 2018.

Draxler, R. R. and Rolph, G. D.: HYSPLIT (HYbrid Single-Particle Lagrangian Integrated Trajectory) Model access via NOAA ARL READY Website, available at: http://ready.arl.noaa.gov/HYSPLIT.php (last access: 23 March 2020), NOAA Air Resources Laboratory, Silver Spring, MD, 2011.

Eerdekens, G., Yassaa, N., Sinha, V., Aalto, P. P., Aufmhoff, H., Arnold, F., Fiedler, V., Kulmala, M., and Williams, J.: VOC measurements within a boreal forest during spring 2005: on the occurrence of elevated monoterpene concentrations during night time intense particle concentration events, Atmos. Chem. Phys., 9, 8331–8350, https://doi.org/10.5194/acp-9-8331-2009, 2009.

Eger, P. G., Helleis, F., Schuster, G., Phillips, G. J., Lelieveld, J., and Crowley, J. N.: Chemical ionization quadrupole mass spectrometer with an electrical discharge ion source for atmospheric trace gas measurement, Atmos. Meas. Tech., 12, 1935–1954, https://doi.org/10.5194/amt-12-1935-2019, 2019.

Eisenreich, W., Rohdich, F., and Bacher, A.: Deoxyxylulose phosphate pathway to terpenoids, Trends Plant Sci., 6, 78–84, https://doi.org/10.1016/s1360-1385(00)01812-4, 2001.

Eugene, A. J. and Guzman, M. I.: Reactivity of ketyl and acetyl radicals from direct solar actinic photolysis of aqueous pyruvic acid, J. Phys. Chem. A, 121, 2924–2935, https://doi.org/10.1021/acs.jpca.6b11916, 2017.

Eugene, A. J. and Guzman, M. I.: The Effects of Reactant Concentration and Air Flow Rate in the Consumption of Dissolved O-2

during the Photochemistry of Aqueous Pyruvic Acid, Molecules, 24, 1124, https://doi.org/10.3390/molecules24061124, 2019.

Eugene, A. J., Pillar, E. A., Colussi, A. J., and Guzman, M. I.: Enhanced Acidity of Acetic and Pyruvic Acids on the Surface of Water, Langmuir, 34, 9307–9313, https://doi.org/10.1021/acs.langmuir.8b01606, 2018.

Fick, J., Pommer, L., Nilsson, C., and Andersson, B.: Effect of OH radicals, relative humidity, and time on the composition of the products formed in the ozonolysis of alpha-pinene, Atmos. Environ., 37, 4087–4096, https://doi.org/10.1016/s1352-2310(03)00522-3, 2003.

Fishman, J. and Crutzen, P. J.: The origin of ozone in the troposphere, Nature, 274, 855, https://doi.org/10.1038/274855a0, 1978.

Folkers, M., Mentel, T. F., and Wahner, A.: Influence of an organic coating on the reactivity of aqueous aerosols probed by the heterogeneous hydrolysis of N_2O_5, Geophys. Res. Lett., 30, 1644, https://doi.org/10.1029/2003GL017168, 2003.

Gaffney, J., Marley, N., Cunningham, M., and Doskey, P.: Measurements of peroxyacyl nitrates (PANS) in Mexico City: implications for megacity air quality impacts on regional scales, Atmos. Environ., 33, 5003–5012, https://doi.org/10.1016/S1352-2310(99)00263-0, 1999.

Graus, M., Muller, M., and Hansel, A.: High Resolution PTR-TOF: Quantification and Formula Confirmation of VOC in Real Time, J. Am. Soc. Mass Spectr., 21, 1037–1044, https://doi.org/10.1016/j.jasms.2010.02.006, 2010.

Griffith, E. C., Carpenter, B. K., Shoemaker, R. K., and Vaida, V.: Photochemistry of aqueous pyruvic acid, P. Natl. Acad. Sci. USA, 110, 11714–11719, https://doi.org/10.1073/pnas.1303206110, 2013.

Grosjean, D.: Atmospheric reactions of pyruvic acid, Atmos. Environ., 17, 2379–2382, https://doi.org/10.1016/0004-6981(83)90242-1, 1983.

Grosjean, D.: Atmospheric reactions of ortho cresol: gas phase and aerosol products, Atmos. Environ., 18, 1641–1652, https://doi.org/10.1016/0004-6981(84)90386-X, 1984.

Grosjean, D., Williams, E. L., and Grosjean, E.: Atmospheric chemistry of isoprene and of its carbonyl products, Environ. Sci. Technol., 27, 830–840, https://doi.org/10.1021/es00042a004, 1993.

Guzman, M. I., Hildebrandt, L., Colussi, A. J., and Hoffmann, M. R.: Cooperative hydration of pyruvic acid in ice, J. Am. Chem. Soc., 128, 10621–10624, https://doi.org/10.1021/ja062039v, 2006.

Hakola, H., Tarvainen, V., Laurila, T., Hiltunen, V., Hellén, H., and Keronen, P.: Seasonal variation of VOC concentrations above a boreal coniferous forest, Atmos. Environ., 37, 1623–1634, https://doi.org/10.1016/S1352-2310(03)00014-1, 2003.

Hakola, H., Hellén, H., and Laurila, T.: Ten years of light hydrocarbons (C2–C6) concentration measurements in background air in Finland, Atmos. Environ., 40, 3621–3630, https://doi.org/10.1016/j.atmosenv.2005.08.019, 2006.

Hakola, H., Hellén, H., Hemmilä, M., Rinne, J., and Kulmala, M.: In situ measurements of volatile organic compounds in a boreal forest, Atmos. Chem. Phys., 12, 11665–11678, https://doi.org/10.5194/acp-12-11665-2012, 2012.

Hallquist, M., Wenger, J. C., Baltensperger, U., Rudich, Y., Simpson, D., Claeys, M., Dommen, J., Donahue, N. M., George, C., Goldstein, A. H., Hamilton, J. F., Herrmann, H., Hoff-

mann, T., Iinuma, Y., Jang, M., Jenkin, M. E., Jimenez, J. L., Kiendler-Scharr, A., Maenhaut, W., McFiggans, G., Mentel, Th. F., Monod, A., Prévôt, A. S. H., Seinfeld, J. H., Surratt, J. D., Szmigielski, R., and Wildt, J.: The formation, properties and impact of secondary organic aerosol: current and emerging issues, Atmos. Chem. Phys., 9, 5155–5236, https://doi.org/10.5194/acp-9-5155-2009, 2009.

Hari, P. and Kulmala, M.: Station for Measuring Ecosystem–Atmosphere Relations (SMEAR II), Boreal Environ. Res., 10, 315–322, https://doi.org/10.1007/978-94-007-5603-8_9, 2005.

Hari, P., Heliövaara, K., and Kulmala, L.: Physical and Physiological Forest Ecology: Physical and Physiological Forest Ecology, edited by: Hari, P., Heliövaara, K., and Kulmala, L., Springer Science & Business Media, Dordrecht, 2013.

Helas, G., Bingemer, H., and Andreae, M. O.: Organic acids over equatorial Africa: Results from DECAFE 88, J. Geophys. Res.-Atmos., 97, 6187–6193, https://doi.org/10.1029/91jd01438, 1992.

Hellén, H., Kouznetsov, R., Anttila, P., and Hakola, H.: Increasing influence of easterly air masses on NMHC concentrations at the Pallas-Sodankylä GAW station, Boreal Environ. Res., 20, 542–552, 2015.

Hellén, H., Praplan, A. P., Tykkä, T., Ylivinkka, I., Vakkari, V., Bäck, J., Petäjä, T., Kulmala, M., and Hakola, H.: Long-term measurements of volatile organic compounds highlight the importance of sesquiterpenes for the atmospheric chemistry of a boreal forest, Atmos. Chem. Phys., 18, 13839–13863, https://doi.org/10.5194/acp-18-13839-2018, 2018.

Hens, K., Novelli, A., Martinez, M., Auld, J., Axinte, R., Bohn, B., Fischer, H., Keronen, P., Kubistin, D., Nölscher, A. C., Oswald, R., Paasonen, P., Petäjä, T., Regelin, E., Sander, R., Sinha, V., Sipilä, M., Taraborrelli, D., Tatum Ernest, C., Williams, J., Lelieveld, J., and Harder, H.: Observation and modelling of HO_x radicals in a boreal forest, Atmos. Chem. Phys., 14, 8723–8747, https://doi.org/10.5194/acp-14-8723-2014, 2014.

Horowitz, A., Meller, R., and Moortgat, G. K.: The UV-VIS absorption cross sections of the alpha-dicarbonyl compounds: Pyruvic acid, biacetyl and glyoxal, J. Photoch. Photobio. A, 146, 19–27, https://doi.org/10.1016/s1010-6030(01)00601-3, 2001.

IUPAC: Task Group on Atmospheric Chemical Kinetic Data Evaluation (Ammann, M., Cox, R. A., Crowley, J. N., Herrmann, H., Jenkin, M. E., McNeill, V. F., Mellouki, A., Rossi, M. J., Troe, J., and Wallington, T. J.), available at: http://iupac.pole-ether.fr/index.html (last access: 23 March 2020), 2019.

Jacob, D. J. and Wofsy, S. C.: Photochemistry of biogenic emissions over the Amazon forest, J. Geophys. Res.-Atmos., 93, 1477–1486, https://doi.org/10.1029/JD093iD02p01477, 1988.

Jardine, K. J., Sommer, E. D., Saleska, S. R., Huxman, T. E., Harley, P. C., and Abrell, L.: Gas Phase Measurements of Pyruvic Acid and Its Volatile Metabolites, Environ. Sci. Technol., 44, 2454–2460, https://doi.org/10.1021/es903544p, 2010.

Jenkin, M. E., Cox, R. A., Emrich, M., and Moortgat, G. K.: Mechanism of the Cl-atom initiated oxidation of acetone and hydroxyacetone in air, J. Chem. Soc. Faraday T., 89, 2983–2991, https://doi.org/10.1039/FT9938902983, 1993.

Jordan, A., Haidacher, S., Hanel, G., Hartungen, E., Mark, L., Seehauser, H., Schottkowsky, R., Sulzer, P., and Mark, T. D.: A high resolution and high sensitivity proton-transfer-reaction time-of-flight mass spectrometer (PTR-TOF-MS), Int. J. Mass Spec-

trom., 286, 122–128, https://doi.org/10.1016/j.ijms.2009.07.005, 2009.

Junninen, H., Lauri, A., Keronen, P., Aalto, P., Hiltunen, V., Hari, P., and Kulmala, M.: Smart-SMEAR: on-line data exploration and visualization tool for SMEAR stations, Boreal Environ. Res., 14, 447–457, 2009.

Kanakidou, M., Seinfeld, J. H., Pandis, S. N., Barnes, I., Dentener, F. J., Facchini, M. C., Van Dingenen, R., Ervens, B., Nenes, A., Nielsen, C. J., Swietlicki, E., Putaud, J. P., Balkanski, Y., Fuzzi, S., Horth, J., Moortgat, G. K., Winterhalter, R., Myhre, C. E. L., Tsigaridis, K., Vignati, E., Stephanou, E. G., and Wilson, J.: Organic aerosol and global climate modelling: a review, Atmos. Chem. Phys., 5, 1053–1123, https://doi.org/10.5194/acp-5-1053-2005, 2005.

Kesselmeier, J. and Staudt, M.: Biogenic volatile organic compounds (VOC): An overview on emission, physiology and ecology, J. Atmos. Chem., 33, 23–88, https://doi.org/10.1023/a:1006127516791, 1999.

Khwaja, H. A.: Atmospheric concentrations of carboxylic acids and related compounds at a semiurban site, Atmos. Environ., 29, 127–139, https://doi.org/10.1016/1352-2310(94)00211-3, 1995.

Kulmala, M., Suni, T., Lehtinen, K. E. J., Dal Maso, M., Boy, M., Reissell, A., Rannik, Ü., Aalto, P., Keronen, P., Hakola, H., Bäck, J., Hoffmann, T., Vesala, T., and Hari, P.: A new feedback mechanism linking forests, aerosols, and climate, Atmos. Chem. Phys., 4, 557–562, https://doi.org/10.5194/acp-4-557-2004, 2004.

Lee, B. H., Lopez-Hilfiker, F. D., Mohr, C., Kurten, T., Worsnop, D. R., and Thornton, J. A.: An Iodide-Adduct High-Resolution Time-of-Flight Chemical-Ionization Mass Spectrometer: Application to Atmospheric Inorganic and Organic Compounds, Environ. Sci. Technol., 48, 6309–6317, https://doi.org/10.1021/es500362a, 2014.

Liebmann, J., Karu, E., Sobanski, N., Schuladen, J., Ehn, M., Schallhart, S., Quéléver, L., Hellen, H., Hakola, H., Hoffmann, T., Williams, J., Fischer, H., Lelieveld, J., and Crowley, J. N.: Direct measurement of NO$_3$ radical reactivity in a boreal forest, Atmos. Chem. Phys., 18, 3799–3815, https://doi.org/10.5194/acp-18-3799-2018, 2018.

Liebmann, J., Sobanski, N., Schuladen, J., Karu, E., Hellén, H., Hakola, H., Zha, Q., Ehn, M., Riva, M., Heikkinen, L., Williams, J., Fischer, H., Lelieveld, J., and Crowley, J. N.: Alkyl nitrates in the boreal forest: formation via the NO$_3$-, OH- and O$_3$-induced oxidation of biogenic volatile organic compounds and ambient lifetimes, Atmos. Chem. Phys., 19, 10391–10403, https://doi.org/10.5194/acp-19-10391-2019, 2019.

Lightfoot, P. D., Cox, R. A., Crowley, J. N., Destriau, M., Hayman, G. D., Jenkin, M. E., Moortgat, G. K., and Zabel, F.: Organic Peroxy-radicals – Kinetics, Spectroscopy and Tropospheric Chemistry, Atmos. Environ. A-Gen., 26, 1805–1961, 1992.

Lopez-Hilfiker, F. D., Mohr, C., Ehn, M., Rubach, F., Kleist, E., Wildt, J., Mentel, Th. F., Lutz, A., Hallquist, M., Worsnop, D., and Thornton, J. A.: A novel method for online analysis of gas and particle composition: description and evaluation of a Filter Inlet for Gases and AEROsols (FIGAERO), Atmos. Meas. Tech., 7, 983–1001, https://doi.org/10.5194/amt-7-983-2014, 2014.

Magel, E., Mayrhofer, S., Müller, A., Zimmer, I., Hampp, R., and Schnitzler, J.-P.: Photosynthesis and substrate supply for isoprene biosynthesis in poplar leaves, Atmos. Environ., 40, 138–151, https://doi.org/10.1016/j.atmosenv.2005.09.091, 2006.

Mattila, J. M., Brophy, P., Kirkland, J., Hall, S., Ullmann, K., Fischer, E. V., Brown, S., McDuffie, E., Tevlin, A., and Farmer, D. K.: Tropospheric sources and sinks of gas-phase acids in the Colorado Front Range, Atmos. Chem. Phys., 18, 12315–12327, https://doi.org/10.5194/acp-18-12315-2018, 2018.

Mekic, M., Liu, J., Zhou, W., Loisel, G., Cai, J., He, T., Jiang, B., Yu, Z., Lazarou, Y. G., Li, X., Brigante, M., Vione, D., and Gligorovski, S.: Formation of highly oxygenated multifunctional compounds from cross-reactions of carbonyl compounds in the atmospheric aqueous phase, Atmos. Environ., 219, 117046, https://doi.org/10.1016/j.atmosenv.2019.117046, 2019.

Mellouki, A. and Mu, Y.: On the atmospheric degradation of pyruvic acid in the gas phase, J. Photoch. Photobio. A, 157, 295–300, https://doi.org/10.1016/S1010-6030(03)00070-4, 2003.

Millet, D. B., Guenther, A., Siegel, D. A., Nelson, N. B., Singh, H. B., de Gouw, J. A., Warneke, C., Williams, J., Eerdekens, G., Sinha, V., Karl, T., Flocke, F., Apel, E., Riemer, D. D., Palmer, P. I., and Barkley, M.: Global atmospheric budget of acetaldehyde: 3-D model analysis and constraints from in-situ and satellite observations, Atmos. Chem. Phys., 10, 3405–3425, https://doi.org/10.5194/acp-10-3405-2010, 2010.

Obermeyer, G., Aschmann, S. M., Atkinson, R., and Arey, J.: Carbonyl atmospheric reaction products of aromatic hydrocarbons in ambient air, Atmos. Environ., 43, 3736–3744, https://doi.org/10.1016/j.atmosenv.2009.04.015, 2009.

Paulot, F., Crounse, J. D., Kjaergaard, H. G., Kroll, J. H., Seinfeld, J. H., and Wennberg, P. O.: Isoprene photooxidation: new insights into the production of acids and organic nitrates, Atmos. Chem. Phys., 9, 1479–1501, https://doi.org/10.5194/acp-9-1479-2009, 2009.

Petäjä, T., Mauldin, III, R. L., Kosciuch, E., McGrath, J., Nieminen, T., Paasonen, P., Boy, M., Adamov, A., Kotiaho, T., and Kulmala, M.: Sulfuric acid and OH concentrations in a boreal forest site, Atmos. Chem. Phys., 9, 7435–7448, https://doi.org/10.5194/acp-9-7435-2009, 2009.

Phillips, G. J., Pouvesle, N., Thieser, J., Schuster, G., Axinte, R., Fischer, H., Williams, J., Lelieveld, J., and Crowley, J. N.: Peroxyacetyl nitrate (PAN) and peroxyacetic acid (PAA) measurements by iodide chemical ionisation mass spectrometry: first analysis of results in the boreal forest and implications for the measurement of PAN fluxes, Atmos. Chem. Phys., 13, 1129–1139, https://doi.org/10.5194/acp-13-1129-2013, 2013.

Pillar, E. A. and Guzman, M. I.: Oxidation of Substituted Catechols at the Air-Water Interface: Production of Carboxylic Acids, Quinones, and Polyphenols, Environ. Sci. Technol., 51, 4951–4959, https://doi.org/10.1021/acs.est.7b00232, 2017.

Pillar, E. A., Camm, R. C., and Guzman, M. I.: Catechol Oxidation by Ozone and Hydroxyl Radicals at the Air-Water Interface, Environ. Sci. Tech., 48, 14352–14360, https://doi.org/10.1021/es504094x, 2014.

Pillar, E. A., Zhou, R. X., and Guzman, M. I.: Heterogeneous Oxidation of Catechol, J. Phys. Chem. A, 119, 10349–10359, https://doi.org/10.1021/acs.jpca.5b07914, 2015.

Pillar-Little, E. A. and Guzman, M. I.: An Overview of Dynamic Heterogeneous Oxidations in the Troposphere, Environments, 5, 104, https://doi.org/10.3390/environments5090104, 2018.

Praplan, A. P., Hegyi-Gaeggeler, K., Barmet, P., Pfaffenberger, L., Dommen, J., and Baltensperger, U.: Online measurements of water-soluble organic acids in the gas and aerosol phase from the photooxidation of 1,3,5-trimethylbenzene, Atmos. Chem. Phys., 14, 8665–8677, https://doi.org/10.5194/acp-14-8665-2014, 2014.

Raber, W. H. and Moortgat, G. K.: Photooxidation of selected carbonyl compounds in air: methyl ethyl ketone, methyl vinyl ketone, methacrolein and methylglyoxal, Progress and problems in atmospheric chemistry, edited by: Barker, JR, World Scientific Publishing, Singapore, 318–373, 1995.

Reed Harris, A. E., Ervens, B., Shoemaker, R. K., Kroll, J. A., Rapf, R. J., Griffith, E. C., Monod, A., and Vaida, V.: Photochemical kinetics of pyruvic acid in aqueous solution, J. Phys. Chem. A, 118, 8505–8516, https://doi.org/10.1021/jp502186q, 2014.

Reed Harris, A. E., Cazaunau, M., Gratien, A., Pangui, E., Doussin, J. F., and Vaida, V.: Atmospheric Simulation Chamber Studies of the Gas-Phase Photolysis of Pyruvic Acid, J. Phys. Chem. A, 121, 8348–8358, https://doi.org/10.1021/acs.jpca.7b05139, 2017.

Rinne, J., Ruuskanen, T. M., Reissell, A., Taipale, R., Hakola, H., and Kulmala, M.: On-line PTR-MS measurements of atmospheric concentrations of volatile organic compounds in a European boreal forest ecosystem, Boreal Environ. Res., 10, 425–436, 2005.

Riva, M., Heikkinen, L., Bell, D. M., Peräkylä, O., Zha, Q., Schallhart, S., Rissanen, M. P., Imre, D., Petäjä, T., Thornton, J. A., Zelenyuk, A., and Ehn, M.: Chemical transformations in monoterpene-derived organic aerosol enhanced by inorganic composition, Climate and Atmospheric Science, 2, 2, https://doi.org/10.1038/s41612-018-0058-0, 2019.

Roberts, J. M.: The atmospheric chemistry of organic nitrates, Atmos. Environ. A-Gen., 24, 243–287, https://doi.org/10.1016/0960-1686(90)90108-y, 1990.

Roberts, J. M., Flocke, F., Stroud, C. A., Hereid, D., Williams, E., Fehsenfeld, F., Brune, W., Martinez, M., and Harder, H.: Ground-based measurements of peroxycarboxylic nitric anhydrides (PANs) during the 1999 Southern Oxidants Study Nashville Intensive, J. Geophys. Res.-Atmos., 107, 4554, https://doi.org/10.1029/2001jd000947, 2002.

Roberts, J. M., Jobson, B. T., Kuster, W., Goldan, P., Murphy, P., Williams, E., Frost, G., Riemer, D., Apel, E., Stroud, C., Wiedinmyer, C., and Fehsenfeld, F.: An examination of the chemistry of peroxycarboxylic nitric anhydrides and related volatile organic compounds during Texas Air Quality Study 2000 using ground-based measurements, J. Geophys. Res.-Atmos., 108, 4495, https://doi.org/10.1029/2003jd003383, 2003.

Rohrer, F. and Berresheim, H.: Strong correlation between levels of tropospheric hydroxyl radicals and solar ultraviolet radiation, Nature, 442, 184–187, https://doi.org/10.1038/nature04924, 2006.

Sihto, S.-L., Mikkilä, J., Vanhanen, J., Ehn, M., Liao, L., Lehtipalo, K., Aalto, P. P., Duplissy, J., Petäjä, T., Kerminen, V.-M., Boy, M., and Kulmala, M.: Seasonal variation of CCN concentrations and aerosol activation properties in boreal forest, Atmos. Chem. Phys., 11, 13269–13285, https://doi.org/10.5194/acp-11-13269-2011, 2011.

Singh, H. B., Kanakidou, M., Crutzen, P. J., and Jacob, D. J.: High concentrations and photochemical fate of oxygenated hydrocarbons in the global troposphere, Nature, 378, 50–54, https://doi.org/10.1038/378050a0, 1995.

Sobanski, N., Schuladen, J., Schuster, G., Lelieveld, J., and Crowley, J. N.: A five-channel cavity ring-down spectrometer for the detection of NO_2, NO_3, N_2O_5, total peroxy nitrates and total alkyl nitrates, Atmos. Meas. Tech., 9, 5103–5118, https://doi.org/10.5194/amt-9-5103-2016, 2016.

Staudinger, J. and Roberts, P. V.: A critical review of Henry's law constants for environmental applications, Crit. Rev. Env. Sci. Tec., 26, 205–297, https://doi.org/10.1080/10643389609388492, 1996.

Stefan, M. I. and Bolton, J. R.: Reinvestigation of the acetone degradation mechanism in dilute aqueous solution by the UV/H_2O_2 process, Environ. Sci. Technol., 33, 870–873, https://doi.org/10.1021/es9808548, 1999.

Talbot, R., Andreae, M., Berresheim, H., Jacob, D. J., and Beecher, K.: Sources and sinks of formic, acetic, and pyruvic acids over Central Amazonia: 2. Wet season, J. Geophys. Res.-Atmos., 95, 16799–16811, https://doi.org/10.1029/JD095iD10p16799, 1990.

Talbot, R. W., Mosher, B. W., Heikes, B. G., Jacob, D. J., Munger, J. W., Daube, B. C., Keene, W. C., Maben, J. R., and Artz, R. S.: Carboxylic acids in the rural continental atmosphere over the eastern United States during the Shenandoah Cloud and Photochemistry Experiment, J. Geophys. Res.-Atmos., 100, 9335–9343, https://doi.org/10.1029/95jd00507, 1995.

Tan, Y., Lim, Y. B., Altieri, K. E., Seitzinger, S. P., and Turpin, B. J.: Mechanisms leading to oligomers and SOA through aqueous photooxidation: insights from OH radical oxidation of acetic acid and methylglyoxal, Atmos. Chem. Phys., 12, 801–813, https://doi.org/10.5194/acp-12-801-2012, 2012.

Vereecken, L., Muller, J. F., and Peeters, J.: Low-volatility poly-oxygenates in the OH-initiated atmospheric oxidation of alpha-pinene: impact of non-traditional peroxyl radical chemistry, Phys. Chem. Chem. Phys., 9, 5241–5248, https://doi.org/10.1039/b708023a, 2007.

Veres, P., Roberts, J. M., Warneke, C., Welsh-Bon, D., Zahniser, M., Herndon, S., Fall, R., and de Gouw, J.: Development of negative-ion proton-transfer chemical-ionization mass spectrometry (NI-PT-CIMS) for the measurement of gas-phase organic acids in the atmosphere, Int. J. Mass Spectrom., 274, 48–55, https://doi.org/10.1016/j.ijms.2008.04.032, 2008.

Veres, P., Gilman, J. B., Roberts, J. M., Kuster, W. C., Warneke, C., Burling, I. R., and de Gouw, J.: Development and validation of a portable gas phase standard generation and calibration system for volatile organic compounds, Atmos. Meas. Tech., 3, 683–691, https://doi.org/10.5194/amt-3-683-2010, 2010.

Warneck, P.: Multi-phase chemistry of C_2 and C_3 organic compounds in the marine atmosphere, J. Atmos. Chem., 51, 119–159, https://doi.org/10.1007/s10874-005-5984-7, 2005.

Williams, J., Crowley, J., Fischer, H., Harder, H., Martinez, M., Petäjä, T., Rinne, J., Bäck, J., Boy, M., Dal Maso, M., Hakala, J., Kajos, M., Keronen, P., Rantala, P., Aalto, J., Aaltonen, H., Paatero, J., Vesala, T., Hakola, H., Levula, J., Pohja, T., Herrmann, F., Auld, J., Mesarchaki, E., Song, W., Yassaa, N., Nölscher, A., Johnson, A. M., Custer, T., Sinha, V., Thieser, J., Pouvesle, N., Taraborrelli, D., Tang, M. J., Bozem, H., Hosaynali-Beygi, Z., Axinte, R., Oswald, R., Novelli, A., Kubistin, D., Hens, K., Javed, U., Trawny, K., Breitenberger, C., Hidalgo, P. J., Ebben, C. J., Geiger, F. M., Corrigan, A. L.,

Russell, L. M., Ouwersloot, H. G., Vilà-Guerau de Arellano, J., Ganzeveld, L., Vogel, A., Beck, M., Bayerle, A., Kampf, C. J., Bertelmann, M., Köllner, F., Hoffmann, T., Valverde, J., González, D., Riekkola, M.-L., Kulmala, M., and Lelieveld, J.: The summertime Boreal forest field measurement intensive (HUMPPA-COPEC-2010): an overview of meteorological and chemical influences, Atmos. Chem. Phys., 11, 10599–10618, https://doi.org/10.5194/acp-11-10599-2011, 2011.

Winterhalter, R., Jensen, N. R., Magneron, I., Wirtz, K., Mellouki, W., Yuying, M., Tadic, J., Horowitz, A., Moortgat, G. K., and Hjorth, J.: Studies of the photolysis of pyruvic acid: Products and mechanism, in: Proceedings of the EUROTRAC-2 Symposium 2000 on "Transport and Chemical Transformation in the Troposphere", edited by: Midgley, P. M., Reuther, M., and Williams, M., Garmisch Partenkirchen, 2000, Springer, Berlin, 2001.

Yu, J. Z., Flagan, R. C., and Seinfeld, J. H.: Identification of products containing −COOH, −OH, and −C=O in atmospheric oxidation of hydrocarbons, Environ. Sci. Technol., 32, 2357–2370, https://doi.org/10.1021/es980129x, 1998.

Zha, Q., Yan, C., Junninen, H., Riva, M., Sarnela, N., Aalto, J., Quéléver, L., Schallhart, S., Dada, L., Heikkinen, L., Peräkylä, O., Zou, J., Rose, C., Wang, Y., Mammarella, I., Katul, G., Vesala, T., Worsnop, D. R., Kulmala, M., Petäjä, T., Bianchi, F., and Ehn, M.: Vertical characterization of highly oxygenated molecules (HOMs) below and above a boreal forest canopy, Atmos. Chem. Phys., 18, 17437–17450, https://doi.org/10.5194/acp-18-17437-2018, 2018.